

An XMM-Newton View of Westerlund 1

P.J. Kavanagh^{1,2}, L. Norci^{1,2}, E.J.A. Meurs^{3,1}

¹School of Physical Sciences, Dublin City University, Glasnevin, Dublin 9, Ireland

²National Centre for Plasma Science and Technology, DCU, Glasnevin, Dublin 9, Ireland

³School of Cosmic Physics, DIAS, 31 Fitzwilliam Place, Dublin 4, Ireland

NCPST
National Centre for Plasma
Science & Technology



Abstract

We present the analysis of a 46 ks XMM-Newton observation of the young Galactic Super Star Cluster (SSC) Westerlund 1. We detect 75 sources in the field. Five of these 75 sources are associated with the cluster. We perform a spectral analysis on the 3 brightest cluster sources (including the well known magnetar) and an analysis of the cluster diffuse emission. We find that the spectral analysis results of the cluster sources and the diffuse emission are in agreement with previous Chandra studies. However, more refined spectral binning for the diffuse emission brings out a Fe 6.7 keV line, indicating a thermal origin for the hard tail of the spectrum.

Introduction

- Initially classified as an open cluster (Westerlund, 1961), Westerlund 1 (Wd1) was found to suffer from significant reddening ($A_V \approx 12.9mag$, Piatti, et al (1998)). Only recently detailed photometric and spectroscopic analyses have been performed (Clark and Negueruela (2002), (2004), Negueruela and Clark (2005), Clark, et al (2005), henceforth CL05, and Brandner et al (2008), henceforth BR08).
- CL05 found rich populations of evolved OB stars and, using a standard Kroupa IMF, inferred an initial cluster mass of $\geq 10^5 M_\odot$. The study of BR08 however used the intermediate and low mass population to calculate the cluster IMF and revised the initial mass estimate to $5.2 \times 10^4 M_\odot$. BR08 also revised previous estimates of age and distance ($3.6(\pm 0.7) Myr$ and $3.55(\pm 0.17) kpc$ respectively) which we adopt for our analysis.
- The large number of evolved stars found by CL05 suggests that Wd1 should contain a rich X-ray population and may exhibit diffuse emission. Analysis of Chandra and XMM-Newton observations of Wd1 have been published (Muno, et al (2006a), Muno, et al (2006b) henceforth MU06, Muno, et al (2007) henceforth MU07, and Clark, et al (2008) henceforth CL08).
- The XMM-Newton data have not been exploited to study the Wd1 cluster as such, but only to examine a magnetar in the cluster (MU07). The aim of our analysis is to use the XMM-Newton data to extract point source and diffuse emission spectra and compare them to those of the published Chandra analysis.

Evolutionary Stage

- For a cluster as massive as Wd1 with a turn off of $\sim 35 M_\odot$ (Clark et al., 2005) we would expect that several supernova (SN) events have already occurred. Indeed, BR08 determine that 63 stars may have undergone a SN event. Despite this, only one source that results from a SN was detected in the cluster by CL08, namely the magnetar.
- Given the turn off, Muno, et al (2006a) conclude the magnetar had a progenitor of $>40 M_\odot$ (CL08 infer a much larger progenitor mass of $55 M_\odot$) which one would expect would form a black hole after the SN event. However, Belczynski and Taam (2008) show that under certain circumstances it is possible for this single neutron star to form from a massive progenitor in a binary system in the Wd1 stellar population.
- We would expect other objects such as High Mass X-ray Binaries (HMXBs) to have formed in the cluster that would be intrinsically brighter than the magnetar and hence be detected by CL08. There are several reasons as to why this is not so. It may be that both the stars in a potential HMXB system have undergone a SN event or that the SN event of one caused a kick velocity resulting in a wider binary configuration in which a HMXB cannot develop.
- Apart from the magnetar, the only objects we can expect to observe in the X-ray are the OB supergiants, Wolf Rayets, Colliding Wind Binaries (CWBs) and low mass pre-main sequence stars detected by CL08.

Observations and Data Reduction

- XMM-Newton observed Wd1 on September 16th 2006 for $\sim 48 ks$ (Muno et al., 2006b) (Obs. ID 0404340101, Revolution 1240). We used the SAS (Version 7.1.0) metatasks *empirc* and *epproc* to produce calibrated event files. We then filtered the data for bad grades and good time intervals as outlined in the SAS User Threads.
- We extracted images from all three EPIC cameras in the 0.3-2 keV, 2-4.5 keV and 4.5-10 keV energy bands and combined these to produce the false colour image shown in Figure 1.

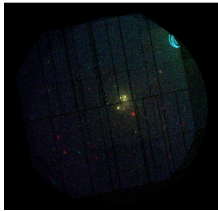


Figure 1: False colour image of Westerlund 1 with red, green and blue corresponding to 0.3-2 keV, 2-4.5 keV and 4.5-10 keV energy bands respectively

- The observation is contaminated with single reflections from a bright source outside the FOV (top right of Figure 1). We find the contaminating object is the low mass X-ray binary 4U 1642-45.
- We applied the SAS metatask *edetect_chain* to detect sources using data from all three EPIC instruments across three energy bands (0.5-2 keV, 2-4.5 keV and 4.5-7.5 keV) to improve sensitivity in the detection of foreground and heavily absorbed sources.
- We detect 90 sources, 7 of which are associated with the reflection and are thus ignored. A further 8 sources were removed after visually identifying them as spurious detections leaving 75 sources in the field, 5 of which are associated with the cluster.

Cluster Point Sources

- Three cluster sources are bright enough to allow spectral analysis. Comparing these source positions to those of CL08 we find that they are:
 - CXOU J164710.2-455216 - the magnetar
 - WR A - WN7b star (CWb system)
 - W 9 and W 30 - sgB[e] star and O9-B0.5 Ia star (sources unresolved by XMM-Newton)

- We extract spectra from PN, MOS1 and MOS2 data and fit them simultaneously in Xspec with several models including the best fit models found in the Chandra studies for the corresponding sources. We find that those models found by CL08 and MU07 best fit the extracted spectra. The spectra and best fits are shown in Figure 2 with the model parameters in Table 1.

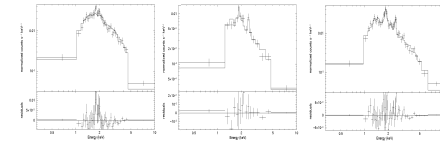


Figure 2: (a) CXOU J164710.2-455216 spectrum and absorbed black-body fit, (b) WR A spectrum with absorbed collisionally ionized plasma fit and (c) combined W 9 and W 30 spectrum with absorbed thermal plasma plus absorbed collisionally ionized plasma fit. For clarity only PN data are shown.

Table 1: Point Source Spectral Parameters

Source Name	N_H	kT	$N_{H,2}$	kT_2	χ^2/ν	$uF_{0.5-10}$	$uL_{0.5-10}$
CXOU J164710.2-455216	$0.90^{+0.02}_{-0.02}$	$0.62^{+0.03}_{-0.03}$	-	-	47.696/44	$3.55^{+0.11}_{-0.11}$	$1.06^{+0.04}_{-0.04}$
WR A	$2.73^{+0.22}_{-0.22}$	$2.40^{+0.10}_{-0.10}$	-	-	28.657/25	$21.8^{+1.1}_{-1.1}$	$6.37^{+0.28}_{-0.28}$
W 30 and W 9	$1.8^{+0.1}_{-0.1}$	$0.7^{+0.1}_{-0.1}$	$2.45^{+0.1}_{-0.1}$	$2.20^{+0.1}_{-0.1}$	128.670/97	$47.4^{+1.1}_{-1.1}$	$14.2^{+0.4}_{-0.4}$

¹ N_H in units of $10^{22} cm^{-2}$, kT in units of keV, $N_{H,2}$ in units of $10^{22} erg cm^{-2} s^{-1}$, $uL_{0.5-10}$ in units of $10^{39} erg s^{-1}$.
² Solar abundances are assumed for all models.
³ We quote unabsorbed X-ray fluxes and luminosities in the 0.5-8 keV energy range to be consistent with the previous works.

- The results are in agreement with the previous studies.

Cluster Diffuse Emission

- It is clear from Figure 1 that there is diffuse emission in the cluster. Diffuse emission can also be seen in the region of the single reflections. To determine the extent of the cluster and reflection diffuse emission we use the Extended Source Analysis Software (ESAS) to create an image of the emission in the MOS1 and MOS2 FOVs as outlined in the ESAS User's Guide.
- We initially ignore residual soft proton contamination and create cheese masks to exclude point sources (including those sources detected by CL08 (source list found at <http://heaarc.gsfc.nasa.gov/W3Browse/chandra/wd1cxo.html>) by excluding pixels within a 5" radius of the source positions). The diffuse emission image is shown in Figure 3.

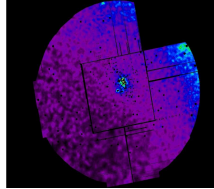


Figure 3: Combined MOS1/MOS2 image of diffuse emission in the FOV. The ccds most affected by the reflection have been omitted.

- We find that the 4U 1642-45 reflection dominates the diffuse emission towards the right of the FOV. Because of this, we cannot determine the true extent of the cluster diffuse emission.
- We used ESAS to generate model particle backgrounds and to extract spectra from regions of interest, however we found the backgrounds to be overestimated (probably because of photons due to the reflection being detected in the unexposed ccd corners).
- Instead, guided by Figure 3, we extract backgrounds from regions that are comparably as contaminated by the reflection as the cluster is. Since this is not very exact, we cannot completely rule out contamination of any diffuse spectra by the single reflections, especially in the outer regions of the cluster.
- We extract MOS1 and MOS2 spectra from the central 1' and 1'-2', 2'-3.5' and 3.5'-5' annuli centered on the cluster core determined by MU06 ($\alpha_0 = 16 47 04.3 \pm 0.1$, $\delta_0 = -45 50 59 \pm 1$), shown in Figure 4. The spectra are binned so that each bin has a S/N of 5.
- MU06 find the spectra are equally well fit with an absorbed two temperature thermal plasma (the harder component with sub-solar abundance) or an absorbed cool thermal plasma plus power law due to a lack of hard emission lines especially the Fe 6.7 keV line at this spectral binning. We fit our spectra with the same models. The spectra are shown in Figure 5 with the fit parameters in Table 2.

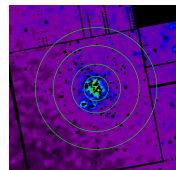


Figure 4: Spectral extraction regions (<1' and 1'-2', 2'-3.5' and 3.5'-5' annuli)

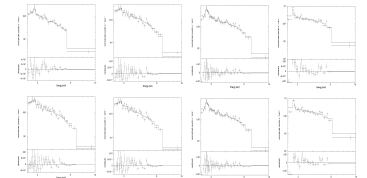


Figure 5: Spectra and absorbed two temperature thermal plasma (top row) and absorbed thermal plasma plus power law (bottom row) fits for <1' and 1'-2', 2'-3.5' and 3.5'-5' annuli (left to right).

Table 2: Diffuse Spectral Parameters

Region	N_H	kT	Two temperature thermal plasma		χ^2/ν	$uF_{0.5-10}$	$uL_{0.5-10}$
			Z/Z_\odot	kT_2			
<1'	$2.03^{+0.10}_{-0.10}$	$0.62^{+0.03}_{-0.03}$	2	$3.43^{+0.10}_{-0.10}$	39.409/52	$4.10^{+0.11}_{-0.11}$	$1.24^{+0.04}_{-0.04}$
1'-2'	$1.73^{+0.08}_{-0.08}$	$0.60^{+0.02}_{-0.02}$	2	$2.86^{+0.10}_{-0.10}$	107.035/89	$7.4^{+0.2}_{-0.2}$	$2.23^{+0.08}_{-0.08}$
2'-3.5'	$2.80^{+0.15}_{-0.15}$	$0.8^{+0.1}_{-0.1}$	2	$2.31^{+0.08}_{-0.08}$	91.093/82	$11.62^{+0.37}_{-0.37}$	$3.47^{+0.12}_{-0.12}$
3.5'-5'	2.42	-	-	3.43	35.632/33	13.6	4.03

Region	N_H	kT	Thermal plasma plus power law		χ^2/ν	$uF_{0.5-10}$	$uL_{0.5-10}$
			Z/Z_\odot	T			
<1'	$2.03^{+0.10}_{-0.10}$	$0.7^{+0.1}_{-0.1}$	2	$2.19^{+0.08}_{-0.08}$	44.847/53	$4.0^{+0.1}_{-0.1}$	$1.20^{+0.04}_{-0.04}$
1'-2'	$1.81^{+0.08}_{-0.08}$	$0.72^{+0.02}_{-0.02}$	2	$2.40^{+0.08}_{-0.08}$	112.406/90	$7.7^{+0.2}_{-0.2}$	$2.32^{+0.08}_{-0.08}$
2'-3.5'	$2.97^{+0.15}_{-0.15}$	$0.8^{+0.1}_{-0.1}$	2	$2.06^{+0.08}_{-0.08}$	91.873/83	$11.0^{+0.3}_{-0.3}$	$3.29^{+0.12}_{-0.12}$
3.5'-5'	2.80	-	-	2.29	35.166/34	16.5	4.04

¹ N_H in units of $10^{22} cm^{-2}$, kT in units of keV, T in units of $10^{10} erg cm^{-2} s^{-1}$, $uL_{0.5-10}$ in units of $10^{39} erg s^{-1}$.
² Z/Z_\odot for both models is fixed at 2 to be consistent with MU06.
³ We quote unabsorbed X-ray fluxes and luminosities in the 2.8-8 keV energy range to be consistent with the previous works.

⁴ In the outermost annulus, the reflection emission becomes a significant part of the background subtracted spectrum. This was modelled with an absorbed power law component in Xspec but since this is poorly constrained the spectral parameters listed above are not reliable.

- As with MU06, we find the spectra are well fit with either model but the two temperature thermal plasma is statistically better in the inner two regions. To assess this further we extract spectra from the inner 2' radius region and bin the spectra so that each bin has a S/N of 3 to make any possible weak and narrow emission lines more obvious. The MU06 spectrum is shown in Figure 6.

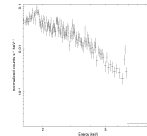


Figure 6: MOS1 <2' spectrum

- The Fe 6.7 keV emission line can now clearly be seen. Fitting this spectrum with the two temperature thermal plasma model yields $N_H = 2.03^{+0.11}_{-0.11} \times 10^{22} cm^{-2}$, $kT_1 = 0.68^{+0.03}_{-0.03}$, $Z/Z_\odot = 2$ (fixed), $kT_2 = 3.07^{+0.07}_{-0.07}$ and $Z/Z_\odot = 0.62^{+0.03}_{-0.03}$. This suggests that the abundance of the hot thermal plasma in the central 2' is higher than that determined by MU06.

Conclusions

- The results from the point source analyses are in agreement with the previous Chandra studies.
- The results from the diffuse emission analysis are in agreement with those of MU06 at comparably coarse binning of the spectra. However, when we combine the inner two extraction regions and refine the S/N of the spectral binning, the Fe 6.7 keV emission line becomes apparent. This suggests that, at least in the inner 2' region, the hard component is thermal in origin, the result of either low mass pre-main sequence stars and/or thermalized winds from the most massive stars in the cluster center.

References

Belczynski, K. and Taam, R.: 2008, *ArXiv e-prints* 804
Brandner, W., Clark, J. S., Stollte, A., Waters, R., Negueruela, I., and Goodwin, S. P.: 2008, *A&A* **478**, 137
Clark, J. S., Muno, M. P., Negueruela, I., Dougherty, S. M., Crowther, P. A., Goodwin, S. P., and de Grijs, R.: 2008, *A&A* **477**, 147
Clark, J. S. and Negueruela, I.: 2002, *A&A* **396**, L25
Clark, J. S. and Negueruela, I.: 2004, *A&A* **413**, L15
Clark, J. S., Negueruela, I., Crowther, P. A., and Goodwin, S. P.: 2005, *A&A* **434**, 949
Muno, M. P., Clark, J. S., Crowther, P. A., Dougherty, S. M., de Grijs, R., Law, C., McMillan, S. L. W., Morris, M. R., Negueruela, I., Pooley, D., Portegies Zwart, S., and Yusef-Zadeh, F.: 2006a, *ApJ* **636**, L41
Muno, M. P., Gaensler, B. M., Clark, J. S., de Grijs, R., Pooley, D., Stevens, I. R., and Portegies Zwart, S. F.: 2007, *MNRAS* **378**, L44
Muno, M. P., Law, C., Clark, J. S., Dougherty, S. M., de Grijs, R., Portegies Zwart, S., and Yusef-Zadeh, F.: 2006b, *ApJ* **650**, 203
Negueruela, I. and Clark, J. S.: 2005, *A&A* **436**, 541
Piatti, A. E., Bica, E., and Claria, J. J.: 1998, *A&AS* **127**, 423
Westerlund, B.: 1961, *PASP* **73**, 51

